Electrostatic force between a charged sphere and a planar surface: A general solution for dielectric materials

Armik Khachatourian, Ho-Kei Chan, Anthony J. Stace, and Elena Bichoutskaia

View Online   Export Citation   CrossMark

ARTICLES YOU MAY BE INTERESTED IN

Electrostatic force between a charged sphere and a planar surface: A general solution for dielectric materials

Armik Khachatourian,[1] Ho-Kei Chan,[2] Anthony J. Stace,[2] and Elena Bichoutskaia[2,a)]
[1]*Department of Physics and Astronomy, California State University, Los Angeles, California 90032-4226, USA*
[2]*Department of Physical and Theoretical Chemistry, School of Chemistry, University of Nottingham, University Park, Nottingham NG7 2RD, United Kingdom*

Using the bispherical coordinate system, an analytical solution describing the electrostatic force between a charged dielectric sphere and a planar dielectric surface is presented. This new solution exhibits excellent numerical convergence, and is sufficiently general as to allow for the presence of charge on both the sphere and the surface. The solution has been applied to two examples of sphere-plane interactions chosen from the literature, namely, (i) a charged lactose sphere interacting with a neutral glass surface and (ii) a charged polystyrene sphere interacting with a neutral graphite surface. Theory suggests that in both cases the electrostatic force makes a major contribution to the experimentally observed attraction at short sphere-plane separations, and that the force is much longer ranged than previously suggested. © *2014 AIP Publishing LLC*. [http://dx.doi.org/10.1063/1.4862897]

I. INTRODUCTION

There are numerous examples[1–7] in science and engineering where improvement in our knowledge of how charged particles interact with a surface could have a significant impact on understanding the mechanisms involved in such interaction and on the possible development of new processes and devices.[1] Examples of where charged particles interact with surfaces are wide ranging and applications include the deposition of inhaled aerosols onto the surface of the lung,[2–4] layer-by-layer powder coating,[5] wet electroscrubbers for gas cleaning,[6] and electrostatic powder coating of food,[7] amongst many others. Particles can acquire charge either by accident or by design, and the question that arises first and foremost is "is the presence of a charge favourable to the process in-hand"? And if the answer is yes, then "what sign and magnitude of charge should the particle accommodate in order to improve performance"? Whilst a number of recent experiments[8–10] have been effective at measuring the forces (electrostatic and van der Waals) between a single charged particle and a surface or substrate, these studies are still restricted to materials that are most amenable to experimentation. Typical of the combinations that have been studied are lactose particles with a glass surface[10] (to mimic tribocharging in particles of pharmaceutical interest) and, as a more general model, polystyrene particles with a graphite surface.[8,9] It is quite possible, therefore, that only an accurate theoretical representation of the interaction of a charged particle with a surface can provide a truly universal picture of events in terms of the range and combination of material and charge that are in need of detailed investigation.[1]

In this study, a general solution describing the interaction between a charged sphere and a planar surface is presented, where both parts are composed of a dielectric material and can carry a charge. The solution provides a measure of the electrostatic force between the two constituents as well as a measure of the redistribution of surface charge that arises as the result of a mutual polarization of the bound charge residing on a particle and on a surface. It is shown that these features of the system are sensitive to the charge and dielectric constant, of both the sphere and the surface.

To date, there have been a number of attempts to model the electrostatic interaction between a charged sphere and a planar surface.[11–16] In most instances, it has been assumed that the sphere and/or the surface are conductors. Nakajima and Sato[13] adapted a dielectric sphere-sphere model by substituting a large sphere for a planar surface, but noted problems with numerical convergence for spheres with substantial differences in radii. The original dielectric sphere-sphere solution,[17] derived in spherical coordinates, diverges at short separations between the interacting spheres if the radius of either sphere is taken to be infinite. To date, some experimental measurements on the force between a particle and a surface have been interpreted using a simple conducting-plane electrostatic model together with additional contributions from van der Waals interactions.[8,9,14] This brief summary suggests that an alternative theoretical approach is required in order to provide a quantitative understanding of the electrostatic interaction between a charged dielectric sphere and a planar dielectric surface.

A general solution for the electrostatic interaction between a pair of charged dielectric spheres derived in bispherical coordinates is shown to be consistent with the previous solution[17] in spherical coordinates. Subsequently, the bispherical solution is adapted to the sphere-plane limit, where it has been used for a numerical study of the interaction between

---
a)Author to whom correspondence should be addressed. Electronic mail: Elena.Bichoutskaia@nottingham.ac.uk; URL: http://bichoutskaia.chem.nottingham.ac.uk.

a charged sphere and a neutral, planar surface. Existing experimental examples of sphere-plane interactions between a charged lactose sphere and a neutral glass surface,[10] and a charged polystyrene sphere with a neutral graphite surface,[8,9] have been investigated, and electrostatic forces and surface-charge densities on both the sphere and the planar surface have been calculated.

II. METHODOLOGY

A. Geometry of the problem in bispherical coordinates

The bispherical coordinate system,[18] as shown in Figure 1, has been employed to calculate the electrostatic force due to the presence of permanent charge residing on the surfaces of two dielectric spheres. Interacting spheres, denoted by i ($i = 1,2$), with an arbitrary radius a_i, permittivity ϵ_i, and carrying an arbitrary charge Q_i, are immersed in a dielectric medium of permittivity $k_m \epsilon_0$ (where for free space $k_m = k_0 = 1$). The permittivity of a sphere relative to that of free space is the dielectric constant $k_i = \frac{\epsilon_i}{\epsilon_0}$, which is dimensionless, where the permittivity of free space (vacuum) ϵ_0 is equal to $8.8541878176 \times 10^{-12}$ F/m. In its normal state, the dielectric material is electrically neutral and contains equal amounts of positive and negative bound (polarization) charge. The free charge on each sphere, which contributes to the net charge of the sphere, is assumed to be distributed uniformly over the surface, such that no volume charge has to be considered. The total surface charge density σ_i is a sum of the free and bound charge densities: $\sigma_i = \sigma_{f,i} + \sigma_{b,i}$. The free charge on each sphere is fixed, independent of the dielectric constant, and does not vary with the separation distance between the spheres. This condition implies a constant free surface charge density, $\sigma_{f,i}$, and the variation in electrostatic force acting on the system is a result of polarization of the bound charge residing on the surface of one sphere induced by an electric field due to the presence of charge on the second sphere.

The position of an arbitrary point X in space is described with reference to inverse-point separations corresponding to spheres 1 and 2, which, like the two foci, are separated by a distance $2a$. As shown in Figure 1(a), c_1 and d_1 are inverse-point separations with respect to sphere 1 ($d_1 c_1 = a_1^2$) and, similarly, c_2 and d_2 are inverse-point separations with respect to sphere 2 ($d_2 c_2 = a_2^2$). The centre-to-centre separation between the interacting spheres is taken to be $h = a_1 + a_2 + s$, where s is the surface-to-surface separation. Alternatively, the separation h can be defined as $h = 2a + c_1 + c_2$, as illustrated also in Figure 1(a).

The bispherical coordinates are denoted as (η, ξ, ϕ) and defined by Arfken[18]

$$x = \frac{a \sin \xi \cos \phi}{\cosh \eta - \cos \xi}; \quad y = \frac{a \sin \xi \sin \phi}{\cosh \eta - \cos \xi};$$

$$z = \frac{a \sinh \eta}{\cosh \eta - \cos \xi}, \tag{1}$$

where η is a dimensionless parameter defined as $\eta = -\ln(\frac{r_1}{r_2})$, and r_1 and r_2 are defined in Figure 1(b); $\eta = \eta_1$ is a positive constant which represents the surface of sphere 1, and $\eta = -\eta_2$ where η_2 is a positive constant which represents the surface of sphere 2. The variable η is, therefore, positive for the upper half plane occupied by sphere 1 ($z \geq 0$ or $0 \leq \theta \leq \frac{\pi}{2}$) and negative for the lower half plane occupied by sphere 2 ($z \leq 0$ or $\frac{\pi}{2} \leq \theta \leq \pi$), the angles θ, θ_1, and θ_2 are defined in Figure 1(b). From the definition of η it follows that $\eta = \infty$ inside sphere 1 when $r_1 = 0$, and $\eta = -\infty$ inside sphere 2 when $r_2 = 0$; on the xy plane ($z = 0$ or $r_2 = r_1$) η is zero.

The z component of Eq. (1) evaluated at the centre of sphere 1, i.e., at $z = z_1$, with $\xi = 0$ and $\xi = \pi$ gives

$$z_1 + a_1 = \frac{a \sinh \eta_1}{\cosh \eta_1 - 1}; \quad z_1 - a_1 = \frac{a \sinh \eta_1}{\cosh \eta_1 + 1}. \tag{2}$$

The angle ξ is defined as $\xi = \theta_1 - \theta_2$, and $\eta = \eta_1$. Equations (2) can be used to express η_1 and a in terms of the position of the center of sphere 1, z_1, and its radius a_1,

$$a = a_1 \sinh \eta_1; \quad z_1 = a \coth \eta_1. \tag{3}$$

It follows that

$$\cosh \eta_1 = \sqrt{1 + \sinh^2 \eta_1} = \sqrt{1 + \frac{a^2}{a_1^2}} \tag{4}$$

and

$$e^{\eta_1} = \frac{a}{a_1} + \sqrt{\left(\frac{a}{a_1}\right)^2 + 1},$$

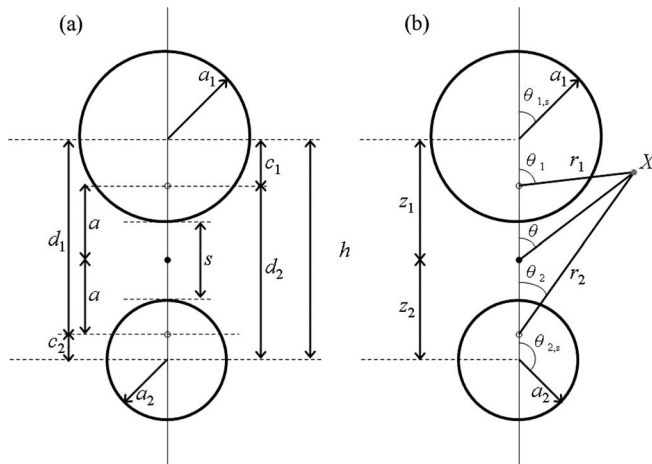$$e^{-\eta_1} = -\frac{a}{a_1} + \sqrt{\left(\frac{a}{a_1}\right)^2 + 1}. \tag{5}$$

FIG. 1. Schematic diagram of the geometric parameters in the bispherical coordinate system: (a) a_1 and a_2 are the radii of sphere 1 and sphere 2; a is half the separation between the two foci; s is the surface-to-surface separation, and h is the centre-to-centre separation; c_1 and d_1 are inverse-point separations with respect to sphere 1 ($d_1 c_1 = a_1^2$), and c_2 and d_2 are inverse-point separations with respect to sphere 2 ($d_2 c_2 = a_2^2$). (b) a position of an arbitrary point X can be described in terms of $\eta \equiv -ln(r_1/r_2)$, $\xi \equiv \theta_1 - \theta_2$, and the azimuthal angle ϕ, where r_1 and r_2 are the distances of the point from the two foci; $\theta_{1,s}$ and $\theta_{2,s}$ are the corresponding polar angles of sphere 1 and sphere 2; θ is the angular position of the point relative to the origin (midpoint of the interfocal separation); z_1 and z_2 are the separations of the centres of sphere 1 and sphere 2 from the origin.

If in (2)–(5) subscript 1 is replaced by 2, these expressions also hold for sphere 2, for which z_2 and η_2 are positive numbers.

The distance a is related to the centre-to-centre separation h by

$$a = \sqrt{\frac{h^4 + (a_1^2 - a_2^2)^2 - 2h^2(a_1^2 + a_2^2)}{4h^2}}. \quad (6)$$

Equations (2)–(5) defined for both spheres 1 and 2, can be used to obtain η_1 and η_2,

$$\cosh \eta_1 = \sqrt{1 + \sinh^2 \eta_1} = \sqrt{1 + \frac{a^2}{a_1^2}} = \frac{h^2 + a_1^2 - a_2^2}{2a_1 h},$$
$$\quad (7)$$
$$\cosh \eta_2 = \sqrt{1 + \sinh^2 \eta_2} = \sqrt{1 + \frac{a^2}{a_2^2}} = \frac{h^2 + a_2^2 - a_1^2}{2a_2 h}.$$

It is also of interest to express the angle ξ in terms of $\theta_{1,s}$ which is the angle that the radial line from the center of sphere 1 makes with the $+z$ axis, which can be found from the z

component of Eq. (1) evaluated on the sphere 1 ($\eta = \eta_1$),

$$z = z_1 + a_1 \cos \theta_{1,s} = \frac{a \sinh \eta_1}{\cosh \eta_1 - \cos \xi} \quad (8)$$

solving Eq. (8) for $\cos \xi$ gives for sphere 1,

$$\cos \xi = \cosh \eta_1 - \frac{a \sinh \eta_1}{z_1 + a_1 \cos \theta_{1,s}}$$
$$= \cosh \eta_1 - \frac{a \sinh \eta_1}{a \coth \eta_1 + a_1 \cos \theta_{1,s}}, \quad (9)$$

where $z_1 = a \coth \eta_1 = a_1 \cosh \eta_1$.

The same derivation can be produced for sphere 2 to obtain

$$\cos \xi = \cosh \eta_2 - \frac{-a \sinh \eta_2}{-a \coth \eta_2 + a_2 \cos \theta_{2,s}}. \quad (10)$$

In the derivation that follows it will be necessary to consider the case where $a_2 \to \infty$ to give a flat planar surface. For a sphere with a radius of a_1 (see Figure 2), the limit $a_2 \to \infty$ for Eq. (6) gives

$$a = \lim_{a_2 \to \infty} \sqrt{\frac{h^4 + (a_1^2 - a_2^2)^2 - 2h^2(a_1^2 + a_2^2)}{4h^2}}$$
$$= \lim_{a_2 \to \infty} \sqrt{\frac{(a_1 + a_2 + s)^4 + (a_1^2 - a_2^2)^2 - 2(a_1 + a_2 + s)^2(a_1^2 + a_2^2)}{4(a_1 + a_2 + s)^2}} = \sqrt{s(s + 2a_1)}, \quad (11)$$

the expression (11) for a is substituted into Eq. (4) to obtain η_1,

$$\eta_1 = \cosh^{-1}\sqrt{1 + \frac{a^2}{a_1^2}} = \cosh^{-1}\left(1 + \frac{s}{a_1}\right) \quad (12)$$

and

$$\eta_2 = 0. \quad (13)$$

From Eq. (1),

$$\rho^2 \equiv x^2 + y^2 = \frac{a^2 \sin^2 \xi}{(\cosh \eta - \cos \xi)^2}$$

on the plane, $\eta = \eta_2 = 0$, and therefore

$$\rho^2 \equiv x^2 + y^2 = \frac{a^2 \sin^2 \xi}{(1 - \cos \xi)^2} = a^2 \frac{1 + \cos \xi}{1 - \cos \xi}$$

hence $\cos \xi$ on the plane takes the following form:

$$\cos \xi = \frac{\rho^2 - a^2}{\rho^2 + a^2} = \frac{\rho^2 - s(s + 2a_1)}{\rho^2 + s(s + 2a_1)}, \quad (14)$$

where the last equality follows by substitution from Eq. (11).

B. Expansion of the electric potential

The electric potential generated at any point in space due to the presence of spheres 1 and 2 is given in Gauss form

$$\Phi(\mathbf{r}) = K \int \frac{dQ}{R} = K \int \frac{dQ_1}{R_1} + K \int \frac{dQ_2}{R_2}, \quad (15)$$

where $K = \frac{1}{4\pi\epsilon_0} \approx 9 \times 10^9$ Vm/C is a constant of proportionality, and the integration is performed over the surfaces of the spheres. The potential $\Phi(\mathbf{r})$ is the sum of the contributions from spheres 1 and 2, and vanishes at infinity. Equation (15)
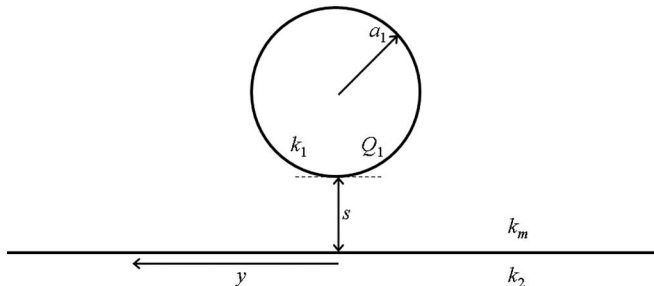

FIG. 2. Schematic diagram of sphere-plane interactions: A sphere of dielectric constant k_1, radius a_1, and net charge Q_1 interacts with a planar surface of dielectric constant k_2 in a medium of dielectric constant k_m.

can be viewed as the time-independent, singular propagator solution of the Poisson two-particle differential equation

$\nabla^2 \psi = -4\pi K \sigma$. The Laplacian in bispherical coordinates has the following form:[19]

$$\nabla^2 = \frac{(\cosh \eta - \cos \xi)^3}{a^2 \sin \xi}$$

$$\times \left[\frac{\partial}{\partial \xi} \left(\frac{\sin \xi}{\cosh \eta - \cos \xi} \frac{\partial}{\partial \xi} \right) + \sin \xi \frac{\partial}{\partial \eta} \left(\frac{1}{\cosh \eta - \cos \xi} \frac{\partial}{\partial \eta} \right) + \frac{1}{\sin \xi [\cosh \eta - \cos \xi]} \frac{\partial^2}{\partial \phi^2} \right].$$

The charge density, σ, resides only on the surface of the sphere, i.e., it is defined by the local charge element on the surface of the sphere, dQ_i.

The local charge element on the surface of the sphere can be expressed as

$$dQ_i = \frac{\sigma_i(\cos \xi') a^2 \sin \xi' d\phi' d\xi'}{(\cosh \eta_i - \cos \xi')^2} \tag{16}$$

and the electric potential (15) takes the form

$$\Phi = K \int_0^\pi \int_0^{2\pi} \frac{\sigma_1(\cos \xi') a^2 \sin \xi' d\phi' d\xi'}{(\cosh \eta_1 - \cos \xi')^2} \frac{1}{R_1} + K \int_0^\pi \int_0^{2\pi} \frac{\sigma_2(\cos \xi') a^2 \sin \xi' d\phi' d\xi'}{(\cosh \eta_2 - \cos \xi')^2} \frac{1}{R_2}. \tag{17}$$

The first term in the electric potential (17) is singular for $\eta = \eta_1$, i.e., when the force field point is on sphere 1. Similarly, the second term is singular for $\eta = -\eta_2$. The inverse distance appearing in each of the integrals in (17) can be further expanded in terms of Legendre polynomials, $P_n(x) = (-1)^n P_n(-x)$, as

$$\frac{1}{R} = \frac{1}{\sqrt{2}a} \frac{\sqrt{\cosh \eta - \cos \xi} \sqrt{\cosh \eta' - \cos \xi'}}{\sqrt{\cosh(\eta - \eta') - (\cos \xi \cos \xi' + \sin \xi \sin \xi' \cos(\phi - \phi'))}}$$

$$= \frac{1}{a} \sqrt{\cosh \eta - \cos \xi} \sqrt{\cosh \eta' - \cos \xi'} \left(\begin{array}{ll} \sum_{n=0}^\infty e^{-(n+\frac{1}{2})(\eta - \eta')} P_n(\cos \psi); & \eta - \eta' > 0 \\ \sum_{n=0}^\infty e^{(n+\frac{1}{2})(\eta - \eta')} P_n(\cos \psi); & \eta - \eta' < 0 \end{array} \right), \tag{18}$$

where $\eta' = \eta_1$ for sphere 1 and $\eta' = -\eta_2$ for sphere 2; $\cos \psi = \cos \xi \cos \xi' + \sin \xi \sin \xi' \cos(\phi - \phi')$. Integration of the inverse distance (18) over the azimuthal angle ϕ' gives

$$\int \frac{d\phi'}{R} = \frac{2\pi}{a} \sqrt{\cosh \eta - \cos \xi} \sqrt{\cosh \eta' - \cos \xi'} \left(\begin{array}{ll} \sum_{n=0}^\infty e^{-(n+\frac{1}{2})(\eta - \eta')} P_n(\cos \xi) P_n(\cos \xi') \\ \sum_{n=0}^\infty e^{(n+\frac{1}{2})(\eta - \eta')} P_n(\cos \xi) P_n(\cos \xi') \end{array} \right). \tag{19}$$

It should be noted that the integration in (19) over the azimuthal angle ϕ' implies that the charge density $\sigma_i(\cos \xi)$ in (16) is independent of ϕ'. Substitution of the expansions (19) in the integral (15) yields a general expression for the electric potential in bispherical coordinates

$$\Phi = K \int \frac{\sigma_1(\cos \xi') a^2 \sin \xi' d\xi'}{(\cosh \eta_1 - \cos \xi')^2} \frac{2\pi}{a} \sqrt{\cosh \eta - \cos \xi} \sqrt{\cosh \eta_1 - \cos \xi'}$$

$$\times \left(\begin{array}{ll} \sum_{n=0}^\infty e^{-(n+\frac{1}{2})(\eta - \eta_1)} P_n(\cos \xi) P_n(\cos \xi'); & \eta - \eta_1 > 0 \\ \sum_{n=0}^\infty e^{(n+\frac{1}{2})(\eta - \eta_1)} P_n(\cos \xi) P_n(\cos \xi'); & \eta - \eta_1 < 0 \end{array} \right)$$

$$+ K \int \frac{\sigma_2(\cos \xi') a^2 \sin \xi' d\xi'}{(\cosh \eta_2 - \cos \xi')^2} \frac{2\pi}{a} \sqrt{\cosh \eta - \cos \xi} \sqrt{\cosh \eta_2 - \cos \xi'}$$

$$\times \left(\begin{array}{ll} \sum_{n=0}^\infty e^{-(n+\frac{1}{2})(\eta + \eta_2)} P_n(\cos \xi) P_n(\cos \xi'); & \eta + \eta_2 > 0 \\ \sum_{n=0}^\infty e^{(n+\frac{1}{2})(\eta + \eta_2)} P_n(\cos \xi) P_n(\cos \xi'); & \eta + \eta_2 < 0 \end{array} \right). \tag{20}$$

The general expression (20) can be simplified if the following coefficients are introduced:

$$\Phi_{i,n} = 2\pi a K \int_0^\pi \frac{\sigma_i(\cos \xi') \sin \xi' d\xi'}{(\cosh \eta_i - \cos \xi')^{\frac{3}{2}}} P_n(\cos \xi'); \quad i = 1, 2. \tag{21}$$

Further substitution of the coefficients $\Phi_{i,n}$ (21) into (20) leads to a simple and more general form of the electric potential

$$\Phi = \sqrt{\cosh\eta - \cos\xi}\sum_{n=0}^{\infty}\Phi_{1,n}P_n(\cos\xi)\begin{pmatrix} e^{-(n+\frac{1}{2})(\eta-\eta_1)}; & \eta-\eta_1 > 0 \\ e^{(n+\frac{1}{2})(\eta-\eta_1)}; & \eta-\eta_1 < 0 \end{pmatrix}$$

$$+ \sqrt{\cosh\eta - \cos\xi}\sum_{n=0}^{\infty}\Phi_{2,n}P_n(\cos\xi)\begin{pmatrix} e^{-(n+\frac{1}{2})(\eta+\eta_2)}; & \eta+\eta_2 > 0 \\ e^{(n+\frac{1}{2})(\eta+\eta_2)}; & \eta+\eta_2 < 0 \end{pmatrix}. \qquad (22)$$

The electric potential inside and outside each sphere can be introduced as $\Phi^{(in)}$ and $\Phi^{(out)}$; more specifically, inside sphere 1 the potential takes the form

$$\Phi_1^{(in)} = \sqrt{\cosh\eta - \cos\xi}\sum_{n=0}^{\infty}\left(\Phi_{1,n}e^{-(n+\frac{1}{2})(\eta-\eta_1)} + \Phi_{2,n}e^{-(n+\frac{1}{2})(\eta+\eta_2)}\right)P_n(\cos\xi), \qquad (23)$$

inside sphere 2

$$\Phi_2^{(in)} = \sqrt{\cosh\eta - \cos\xi}\sum_{n=0}^{\infty}\left(\Phi_{1,n}e^{(n+\frac{1}{2})(\eta-\eta_1)} + \Phi_{2,n}e^{(n+\frac{1}{2})(\eta+\eta_2)}\right)P_n(\cos\xi), \qquad (24)$$

and outside both spheres

$$\Phi^{(out)} = \sqrt{\cosh\eta - \cos\xi}\sum_{n=0}^{\infty}\left(\Phi_{1,n}e^{(n+\frac{1}{2})(\eta-\eta_1)} + \Phi_{2,n}e^{-(n+\frac{1}{2})(\eta+\eta_2)}\right)P_n(\cos\xi)$$

$$= \Phi_1^{(out)} + \Phi_2^{(out)}. \qquad (25)$$

The total charge on each sphere can be found by integrating over all angles as follows:

$$Q_{i,tot} = \int_0^{\pi}\int_0^{2\pi}\frac{\sigma_i(\cos\xi)a^2\sin\xi\,d\phi\,d\xi}{(\cosh\eta_i - \cos\xi)^2}$$

$$= \frac{\sqrt{2}a}{K}\sum_{n=0}^{\infty}\Phi_{i,n}e^{-(n+\frac{1}{2})\eta_i}, \qquad (26)$$

where the last equality follows from Eq. (21).

C. Distribution of the surface charge and application of the boundary conditions

Using the orthogonality of Legendre polynomials, the surface charge density, σ_i, can be obtained from Eq. (21) for sphere 1 as follows:

$$\sigma_1(\cos\xi) = \frac{(\cosh\eta_1 - \cos\xi)^{\frac{3}{2}}}{4\pi Ka}\sum_{n=0}^{\infty}(2n+1)\Phi_{1,n}P_n(\cos\xi) \qquad (27)$$

and for sphere 2,

$$\sigma_2(\cos\xi) = \frac{(\cosh\eta_2 - \cos\xi)^{\frac{3}{2}}}{4\pi Ka}\sum_{n=0}^{\infty}(2n+1)\Phi_{2,n}P_n(\cos\xi), \qquad (28)$$

where $\cos\xi$ is defined by Eqs. (9) and (10).

The boundary conditions applied are identical to those used previously in the spherical coordinate solution.[17] Apart

from the condition that the electric potential vanishes at infinity (except for the case of a charged infinite plane), three additional boundary conditions are applied, and shown here using the surface of sphere 1 as an example. The first boundary condition is continuity of the potential on the surface of the sphere due to continuity of the tangential component of the electric field

$$-\frac{1}{r_s}\frac{\partial\Phi}{\partial\theta_{1,s}}\bigg|_{r_s=a_1^-} = -\frac{1}{r_s}\frac{\partial\Phi}{\partial\theta_{1,s}}\bigg|_{r_s=a_1^+}, \qquad (29)$$

where a_1^+ indicates a point on the outside of the sphere's surface, and a_1^- indicates a point on inside of the sphere's surface. Note that the potential on the surface of the spheres is not constant. The second boundary condition is discontinuity of the normal component of the electric field due to the presence of a net charge on the surface of each sphere

$$4\pi K\sigma_1 = \frac{\partial\Phi}{\partial r_s}\bigg|_{r_s=a_1^-} - \frac{\partial\Phi}{\partial r_s}\bigg|_{r_s=a_1^+}. \qquad (30)$$

Boundary conditions (29) and (30) are automatically satisfied by the choice of electric potential described by Eq. (15).

The last boundary condition states that the normal component of the dielectric displacement field due to the presence of free charge on the surface of a sphere is discontinuous

$$4\pi K\sigma_{f,1} = k_1\frac{\partial\Phi}{\partial r_s}\bigg|_{r_s=a_1^-} - k_m\frac{\partial\Phi}{\partial r_s}\bigg|_{r_s=a_1^+} = \text{constant}. \qquad (31)$$

Eliminating $\left.\frac{\partial \Phi}{\partial r_s}\right|_{r_s=a_1^-}$ from Eqs. (30) and (31) and transforming to bispherical coordinate system gives

$$4\pi K \sigma_1 = 4\pi K \frac{\sigma_{1,f}}{k_1} + \left(\frac{k_m}{k_1} - 1\right) \frac{\cosh\eta - \cos\xi}{-a} \left.\frac{\partial \Phi^{(out)}}{\partial \eta}\right|_{\eta=\eta_1^+}. \tag{32}$$

$$\frac{\sqrt{2}\,a\sigma_{1,f}\,e^{-(n+\frac{1}{2})\eta_1}}{\epsilon_0}$$
$$= \left(\left[\left(n+\frac{1}{2}\right)\Phi_{1,n}\cosh\eta_1 - \frac{n}{2}\Phi_{1,n-1} - \frac{n+1}{2}\Phi_{1,n+1}\right](k_m+k_1) + \frac{\sinh\eta_1}{2}(k_m-k_1)\Phi_{1,n}\right)$$
$$+ \left(-\left[\left(n+\frac{1}{2}\right)\Phi_{2,n}f_n\cosh\eta_1 - \frac{n}{2}\Phi_{2,n-1}f_{n-1} - \frac{n+1}{2}\Phi_{2,n+1}f_{n+1}\right](k_m-k_1) + \Phi_{2,n}f_n\frac{\sinh\eta_1}{2}(k_m-k_1)\right), \tag{33}$$

where the distance a is defined by Eq. (6), the coefficients $\Phi_{i,n}$ are given by Eq. (21), and

$$f_n = e^{-(n+\frac{1}{2})(\eta_1+\eta_2)}. \tag{34}$$

Using the same expansion of the electric potential (25) for sphere 2 and applying the corresponding boundary conditions, as described above for the case of sphere 1, a complementary expression for the coefficients of the potential is obtained, which must follow from Eq. (33) by interchanging subscripts 1 and 2.

D. The electrostatic force

The electrostatic force on sphere 1 due to the presence of net electric charges residing on the surface of sphere 2 can now be readily expressed as

$$\mathbf{F}_{12} = K \int dQ_1(\mathbf{x}) \int dQ_2(\mathbf{x_2}) \frac{\mathbf{x} - \mathbf{x_2}}{|\mathbf{x} - \mathbf{x_2}|^3}$$
$$= -K \int dQ_1(\mathbf{x}) \nabla \left(\int dQ_2(\mathbf{x_2}) \frac{1}{|\mathbf{x} - \mathbf{x_2}|}\right)$$
$$= -\int dQ_1(\mathbf{x})\hat{\mathbf{z}}\frac{\partial}{\partial z}\left(K \int dQ_2(\mathbf{x_2}) \frac{1}{|\mathbf{x} - \mathbf{x_2}|}\right)$$
$$= -\hat{\mathbf{z}} \int dQ_1 \frac{\partial \Phi_2^{(out)}}{\partial z}, \tag{35}$$

where the third equality is due to cylindrical symmetry of the problem, and the convention of a negative term for an attractive contribution to the force and a positive term describing repulsion is used. The first integral takes into account the total charge residing on sphere 1, and the second integral is the potential generated by the total charge residing on sphere 2. The electric potential $\Phi_2^{(out)}$, generated by all charges residing on sphere 2, is given by Eq. (25).

Note that $\frac{\partial}{\partial n} = \hat{\eta}\cdot\vec{\nabla} = \frac{1}{h_\eta}\frac{\partial}{\partial \eta} = \frac{\cosh\eta - \cos\xi}{a}\frac{\partial}{\partial \eta}$. The minus sign is necessary since η inside sphere 1 has a larger value than when outside sphere 1, whereas the opposite is true for sphere 2.

Substitution of Eqs. (25) and (27) on the left and right side of Eq. (32) leads to the following expression for the coefficients of the potential (after equating the coefficients of the Legendre polynomials and further simplifications)

Transformation of the above equation to bispherical coordinate system gives

$$\mathbf{F}_{12} = -\hat{\mathbf{z}} \int dQ_1 \left(\frac{1 - \cos\xi\cosh\eta}{a}\frac{\partial}{\partial \eta} - \frac{\sin\xi\sinh\eta}{a}\frac{\partial}{\partial \xi}\right)\Phi_2^{(out)}\Bigg|_{\eta=\eta_1}, \tag{36}$$

where dQ_i is defined by Eq. (16).

Substituting the electric potential $\Phi_2^{(out)}$, given by Eq. (25), into (36) leads to the following final expression for the electrostatic force (after the integration and some further simplifications),

$$\mathbf{F}_{12} = -\hat{\mathbf{z}} \int_0^\pi \frac{\sigma_1(\cos\xi)a^2\sin\xi\,d\xi}{(\cosh\eta_1 - \cos\xi)^2} 2\pi \frac{\sqrt{\cosh\eta_1 - \cos\xi}}{a} \sum_{n=0}^\infty$$
$$\times f_n \left(\frac{n}{2}P_{n-1}(\cos\xi)e^{\eta_1} - \left(n+\frac{1}{2}\right)P_n(\cos\xi)\right.$$
$$\left.+ \frac{n+1}{2}P_{n+1}(\cos\xi)e^{-\eta_1}\right)\Phi_{2,n}$$
$$= -\frac{1}{K}\hat{\mathbf{z}}\sum_{n=0}^\infty f_n\left(\frac{n}{2}\Phi_{1,n-1}e^{\eta_1}\right.$$
$$\left.- \left(n+\frac{1}{2}\right)\Phi_{1,n} + \frac{n+1}{2}\Phi_{1,n+1}e^{-\eta_1}\right)\Phi_{2,n}$$
$$= \hat{\mathbf{z}}\sum_{n=0}^\infty (F_{n-1,n} + F_{n,n} + F_{n+1,n}), \tag{37}$$

where for the individual terms

$$F_{m,n} \propto \Phi_{1,m}\Phi_{2,n}, \tag{38}$$

m takes on $n-1$, n or $n+1$. Using the aforementioned boundary conditions, $\Phi_{1,m}$ and $\Phi_{2,n}$ can be expressed in

terms of $\sigma_{1,f}$ and $\sigma_{2,f}$ in the following form:

$$\Phi_{1,m} = A\sigma_{1,f} + B\sigma_{2,f},$$

$$\Phi_{2,n} = C\sigma_{1,f} + D\sigma_{2,f}. \tag{39}$$

Thus $F_{m,n}$ is given by

$$F_{m,n} \propto \Phi_{1,m}\Phi_{2,n}$$

$$\propto (A\sigma_{1,f} + B\sigma_{2,f})(C\sigma_{1,f} + D\sigma_{2,f})$$

$$\propto AC\sigma_{1,f}^2 + BD\sigma_{2,f}^2 + (AD + BC)\sigma_{1,f}\sigma_{2,f}, \tag{40}$$

which implies

$$F_{m,n} \propto \sigma_{1,f}^2 \tag{41}$$

for a neutral plane of $\sigma_{2,f} = 0$. It follows that, for the interaction of a charged sphere with a neutral planar surface,

$$\mathbf{F}_{12} \propto \sigma_1^2 \propto Q_1^2. \tag{42}$$

III. COMPARISON BETWEEN THE SOLUTIONS IN SPHERICAL AND BISPHERICAL COORDINATES

In order to validate the new solution, a comparison has been made between electrostatic forces calculated using the spherical coordinate and the bispherical coordinate solutions. For this purpose, an example has been taken from cloud physics,[20–23] and the electrostatic force between a pair of charged water droplets ($k_1 = k_2 = 80$) in air or vacuum ($k_m = 1$) has been calculated. Each droplet carries an identical charge of 200 e, but they have different radii: $a_1 = 1000$ nm and $a_2 = 2500$ nm. Table I shows numerical results calculated using the two different coordinate systems, and as noted earlier,[24] the calculated force is negative at short separations, which implies that the two like-charged spheres are attracted to one another. As shown by this example, results from the two different coordinate systems agree very well: an agreement in the absolute value of the electrostatic force up to at least 5 decimal places has been achieved for short surface-to-surface separations (less than 200 nm), and at separation distances of 300 nm and greater the level of agreement increases to 10 decimal places. At 300 nm, the like-charged

TABLE I. Comparison of theoretical solutions for the electrostatic force between two like-charged spheres obtained in spherical[17] and bispherical (present work) coordinate systems. Parameters for sphere 1 are: charge $Q_1 = 200$ e, radius $a_1 = 1000$ nm, dielectric constant $k_1 = 80$; and for sphere 2: charge $Q_2 = 200$ e, radius $a_2 = 2500$ nm, and dielectric constant $k_2 = 80$. The medium is vacuum with a dielectric constant $k_m = 1$. There are 50 and 110 terms in the Legendre polynomial expansions for the spherical and bispherical solutions, respectively.

Surface-to-surface separation	$\mathbf{F}_{12}$ (pN)	
s (nm)	Spherical solution[17]	Bispherical solution
100	-1.4234709746	-1.4234718673
200	-0.6514501823	-0.6514501829
300	-0.3271645335	-0.3271645335
1000	$+0.1915076788$	$+0.1915076788$
10 000	$+0.0498774468$	$+0.0498774468$

TABLE II. Convergence test for Eq. (37) calculating the electrostatic force, $\mathbf{F}_{12}$. Column 1 shows the surface-to-surface separation, s, relative to the radius a_1 of sphere 1, and column 2 shows the number of terms, n, in the summation of Eq. (37) required to achieve an accuracy of two decimal places in the electrostatic force.

Surface-to-surface separation ($\frac{s}{a_1}$)	Number of terms in expansion (37) (n)
10	2
1	10
0.1	100
0.01	1000

spheres continue to attract one another, but as their separation increases Coulomb repulsion begins to dominate and they start to repel one another. This repulsion continues to make its presence felt even when the surface-to-surface separation reaches 10 000 nm. Although the bispherical solution offers a level of precision which is comparable to that achieved using spherical coordinates, it can be seen from Table I that the number of terms required in the Legendre-polynomial expansion in bispherical coordinates is greater than that for the corresponding expansion in spherical coordinates.

The results presented in Table I show that the bispherical coordinate solution presented here achieves excellent convergence when compared with the earlier spherical coordinate solution,[17] for which convergence criteria have already been established.[17] However, what is most significant in the context of this work is that convergence of the bispherical coordinate solution still holds at the sphere-plane ($a_2 \rightarrow \infty$) limit, where previously numerical problems have been encountered in the spherical coordinate solution[17] when the radius of either sphere was taken to be infinite. In the presented bispherical coordinate solution, the number of elements in the matrix defining a cut-off for the evaluation of the electrostatic force is only $6n$, and as the matrix is diagonally dominant it can be inverted efficiently. A criterion on the selection of the number of terms, n, to be included in order to achieve convergence of the electrostatic force up to two decimal places is presented in Table II.

IV. APPLICATIONS

Recent development of the atomic force microscope (AFM) technique, which can be broadly classified as either static or dynamic,[9] has led to measurements of nano Newton interaction forces between individual micrometer-size spherical objects and atomically flat substrates.[8–10,25] It is generally assumed that the attractive interaction force between an AFM tip and substrate has two components: a long-range electrostatic force and a van der Waals force, where the latter is believed to be dominant at short sphere-substrate separations. However, for a number of reasons, quantitative identification and separation of these contributions to the interaction force is notoriously difficult. First, it is difficult to control and fully characterize the exact geometry and associated charge distribution of the AFM tip (and hence quantify the electrostatic charging); however the ambiguities in the

geometry of the interacting objects can be minimized by means of attaching a micrometer-size particle directly onto an AFM canteliver.[26, 27] Second, separation of the electrostatic and van der Waals components to the interaction force requires the use of different AFM techniques at short and long separations between the tip and the substrate.[9] The static mode of AFM operation, which measures directly the force between a particle mounted on the cantilever and substrate, is mainly suited for long-range measurements. The dynamic mode of AFM operation, on the other hand, estimates the force gradient using a frequency modulation method and is better suited for the measurement of very weak interaction forces. Application of these AFM techniques assume that the electrostatic forces: (a) are predominantly long-ranged and therefore they can be eliminated or even ignored at short separation distances; (b) can be quantitatively understood and interpreted using basic Coulomb models. In fact, both assumptions are too simplistic. The aim of this section is to provide a rigorous assessment as to whether or not electrostatic interactions make a major contribution to the attractive force measured at short sphere-plane separations.

Two well-studied experimental examples of electrostatic force measurements between a charged sphere and a neutral, planar surface have been employed in a numerical study, where the bispherical solution presented in Sec. II has been used. These examples are: (i) the electrostatic force between a positively charged polystyrene sphere and a neutral graphite surface;[8,9] (ii) the electrostatic force between a positively charged lactose sphere and a neutral glass surface.[10] In both cases, AFM measurements[8–10] have revealed an attractive force between the sphere and the planar surface at short separations, where this attraction has been attributed to a combination of electrostatic and van der Waals interactions. In our calculations, the medium between the sphere and the planar surface is taken to be vacuum with a dielectric constant of $k_m = 1$ (see Figure 2 for a schematic diagram illustrating the geometry of the problem). For each example, the electrostatic force has been calculated as a function of the surface-to-surface separation, s, between the sphere and the planar surface using parameters summarized in Table III. The dependence of the force on the square of the charge Q_1, as predicted by Eq. (42), has also been investigated. In addition, the surface density of total charge has been calculated as a function of both the radial position y for the plane and the polar angle $\theta_{1,s}$ for the sphere (see Figures 1 and 2).

For the interaction between polystyrene particle and graphite surface the electrostatic force has been calculated (Figure 3(a)) for a sphere of charge $Q_1 = 10\,000$ e and radius $a_1 = 3000$ nm (experimental values[9]) and compared with other theoretical models. The electrostatic force, shown as curve (b1) in Figure 3(b), between a grounded conducting surface and a sphere of radius 3 μm with a charge of $Q_1 = 10\,000$ e is grossly underestimated at short separations.[9] The model presented in this work, shown as curve (b2) in Figure 3(b), which assumes a uniform distribution of free charge on the surface of each sphere, predicts a much longer range of the electrostatic force than the empirical models[9] used to calculate the force between a conducting surface and a sphere on which the charge is local-
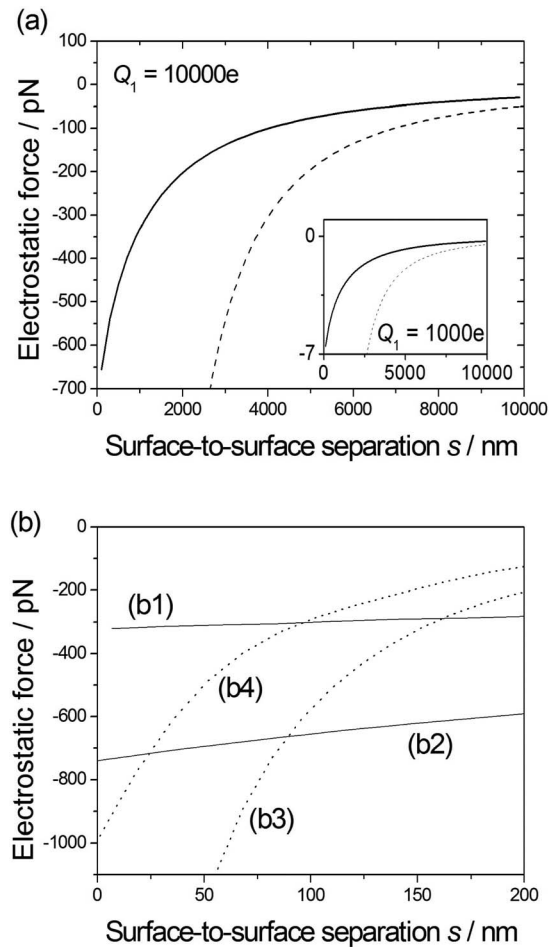

FIG. 3. Electrostatic force, F, between a positively charged polystyrene sphere and a neutral graphite surface in vacuum ($k_m = 1$). (a) The calculated electrostatic force (solid line) as a function of the surface-to-surface separation, s, for a net charge of $Q_1 = 10\,000$ e on the polystyrene sphere. The solid line in the inset corresponds to the electrostatic force calculated for $Q_1 = 1000$ e, and it demonstrates the predicted Q^2-dependence of the force between a charged sphere and a neutral planar surface. The dashed lines represent the image charge model solution for a point charge and conducting surface. (b) Comparison of theoretical results: (b1) the electrostatic force between a grounded conducting surface and a sphere of radius 3 μm with a charge of $Q_1 = 10\,000$ e;[9] (b2) the calculated electrostatic force between a dielectric surface (graphite) and a sphere (polystyrene) of radius 3 μm with a charge of $Q_1 = 10\,000$ e (present work); (b3) the electrostatic force between a grounded conducting surface and a sphere of radius 3 μm with a charge of (b3) but with the effective radius of $R_{eff} = 120$ nm.[9]

ized over a certain effective radius (curves (b3) and (b4) in Figure 3(b)).

For the lactose particle-glass electrostatic interaction, the electrostatic force has been calculated (Figure 4) for a sphere of the estimated charge $Q_1 = 1.66 \times 10^5$ e (no experimental data for the charge on lactose particle is available) and radius $a_1 = 5000$ nm (experimental value[10]). The value of Q_1 used in the calculations of the force lies within the allowed range of experimental charges as it is two orders of magnitude smaller than the value of the maximum possible negative charge (-1.56×10^7 e) and three orders of magnitude smaller than that of the maximum positive charge (3.65 $\times 10^8$ e).[29] As shown in Figure 4(b), at short separation distances the calculated force is comparable in magnitude with the experimental electrostatic force[10] measured immediately

TABLE III. The values of the dielectric constants, k_1 (sphere) and k_2 (plane), and the sphere radius, a_1, for the studied applications of polystyrene-graphite and lactose-glass interactions.

Interacting object	Dielectric constant	Radius (nm)
Polystyrene sphere	$k_1 = 2.6$	$a_1 = 3000$
Graphite surface	$k_2 = 12.0$	
Lactose sphere	$k_1 = 6.0$	$a_1 = 5000$
Glass surface	$k_2 = 2.0$	

after tribocharging at the relative humidity of RH = 0.1%. However, the experimental force decays much faster with the separation distance than the calculated result. Experiments[10] for the lactose-glass example suggest a sensitive dependence of the electrostatic force on relative humidity (RH): as RH increases, the electrostatic force drops sharply, which might have been caused by a loss of charge to water vapour and water ions in humid air,[29] as well as the electrostatic screening of the force by water (dielectric constant = 80). These con-

FIG. 4. Electrostatic force, F, between a positively charged lactose sphere and a neutral glass surface in vacuum ($k_m = 1$). The calculated electrostatic force (solid line) as a function of the surface-to-surface separation, s, for a net charge of $Q_1 = 1.66 \times 10^5$ e on the lactose sphere is shown as solid line; the dashed line in (a) corresponds to the image charge model solution for a point charge; the dotted line in (b) corresponds to an extraction of experimental data from Bunker *et al.*[10] The fast decay of the measured force with the separation distance as compared to the present theoretical data (solid line) is thought to be related to the relative humidity of air in the experiment.

siderations might account for the discrepancy between experiment and theory as the calculated force corresponds to zero RH. However, experiments[10] also show that charge generated on the surface decays with time, and the contributions from charge decay and RH effects have not been separated.

In both examples, the electrostatic force between a charged sphere and a neutral plane is attractive at all separations (see Figures 3 and 4 for the polystyrene-graphite and lactose-glass examples, respectively) as it arises from anisotropies in the induced multipole interactions. The obtained numerical results are in agreement with Eq. (42) for the Q_1^2 dependence of the electrostatic force F between a charged sphere and a neutral plane. As illustrated in the inset of Figure 3(a), with $s \to 0$ the limiting value of the force drops by a factor of 100, from 650 pN to 6.5 pN, if the charge Q_1 decreases by a factor of 10, from 10 000 e to 1000 e. At large separation distances, the calculated electrostatic force is in excellent quantitative agreement with the results obtained for a point charge using the image charge model.[28] As demonstrated in both Figures 3(a) and 4(a), the presented bispherical coordinates solution for a finite size sphere and the corresponding image charge solution for a point charge[28] given by

$$\mathbf{F}_{12} = \frac{1}{4\pi\varepsilon_o}\frac{Q_1}{(2s)^2}\left[\frac{Q_1(1 - k_2)}{(1 + k_2)}\right] \qquad (43)$$

approach a quantitative agreement at large separation distances. The Q_1^2 dependence of the force, as predicted by the presented bispherical solution, becomes immediately clear from the image charge solution (43). At the point charge limit, the electrostatic force is always attractive for a neutral but polarizable planar surface (such as those described in the experimental examples considered here), because the sign of the image point charge is opposite to that of its real counterpart. This accounts for the absence of the attraction-repulsion transition in the electrostatic interaction which occurs, for example, between a pair of charged polarizable spheres[17] or between a charged sphere and a charged surface.

The results presented in this section suggest that the electrostatic force makes a major contribution to the short-range attraction force between a charged sphere and a planar surface, and that this attraction arises from the induced polarization of bound charge on both the surface and the sphere. In the vicinity of a positively charged sphere, a negative polarization charge is induced on the neutral plane, and the effect is most noticeable at the point closest to the sphere's surface, i.e., at $y = 0$. This effect is illustrated in Figure 5 by the example of a positively charged polystyrene sphere interacting with a neutral graphite surface, where the charge distribution on the graphite surface is plotted as a function of the radial position y (Figure 5(a)). It can be seen that the charge density at $y = 0$ is most negative. The induced negative charge on the planar surface, in turn, induces polarization of charge on the surface of polystyrene sphere (Figure 5(b)) so that the density of positive charge is highest at the point on the sphere closest to the planar surface, i.e., at a polar angle of $\theta_{1,s} = \pi$ (Figure 2). For a given value of surface-to-surface separation, the mutual polarization of bound charge continues until the system reaches equilibrium, where the equilibrium state
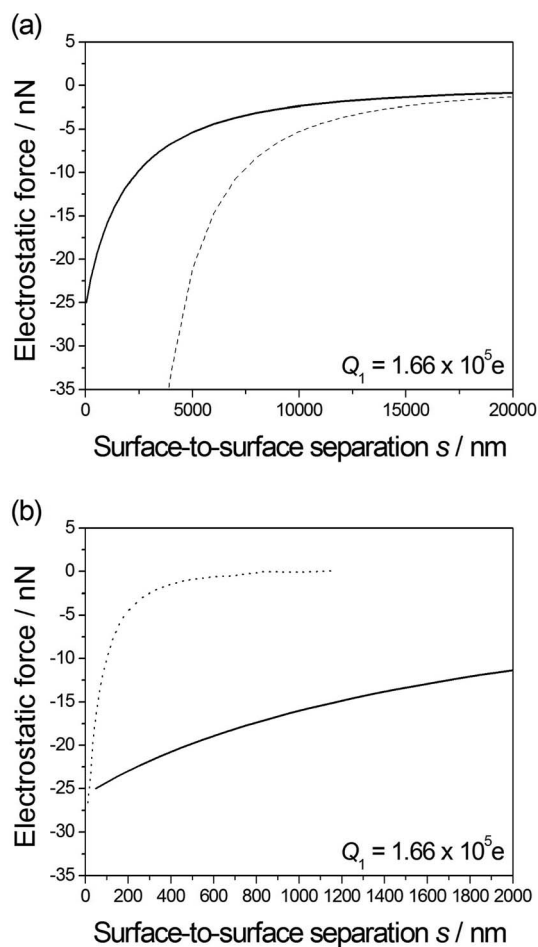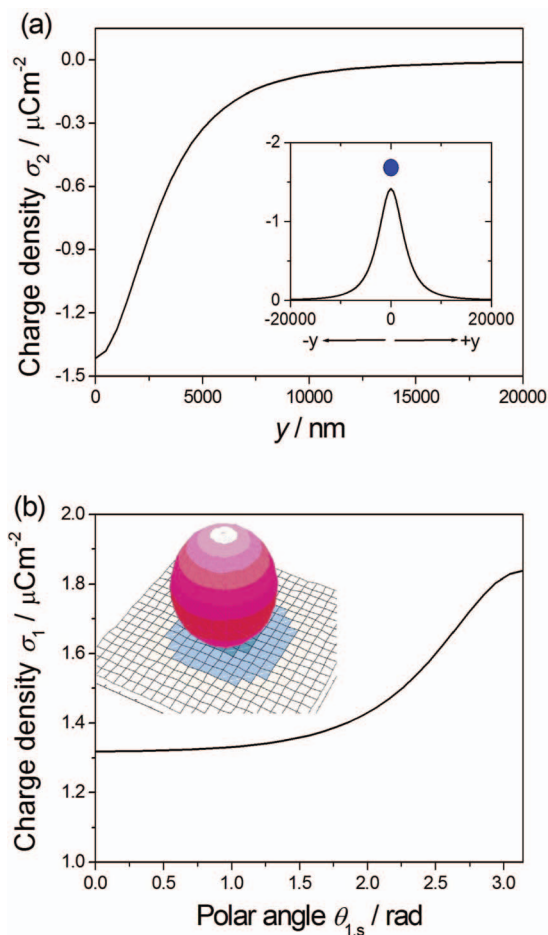
FIG. 5. Charge distribution on the surface of polystyrene sphere ($Q_1 = 1000$ e) and planar, neutral surface of graphite, which are separated by $s = 1100$ nm: (a) the surface density of total charge on the graphite surface as a function of the radial position y; the inset illustrates the distribution of the charge density in the radial direction; (b) the surface density of total charge on the polystyrene sphere as a function of the polar angle $\theta_{1,s}$.

is described in quantitative detail by the theoretical solution presented here.

V. CONCLUSIONS

A general solution for the electrostatic force between two charged, dielectric spheres has been derived using bispherical coordinates and has been shown to be consistent with an earlier solution[17] obtained using spherical coordinates. An advantage of the new bispherical coordinate solution is that, by assigning one sphere an infinite radius, it is readily adapted to the case of a charged dielectric sphere interacting with a planar dielectric surface. Numerical results show that, if the space (medium) between a charged sphere and a neutral planar surface is vacuum, the electrostatic force between the two entities is attractive at all separations. This result suggests that an electrostatic force is one of the main components to the short-range attraction between a charged sphere and a surface. However, what the calculations also reveal (see, for example, Figure 3(a)) is that the electrostatic attraction between a

charged sphere and a neutral surface extends out to a surface-to-surface separation of at least 10 000 nm (10 μm), which is more than three times the radius of the sphere and is much further than what has been determined from experimental results. The calculations suggest that attraction arises from the induced polarization of bound charge on both the sphere and the surface. Therefore, the discrepancies between theory and experiment, as observed for both experimental examples, might have also been contributed from a decay of surface charge on the spheres.

[1] M. K. Mazumder, R. A. Sims, A. S. Biris, P. K. Srirama, D. Saini, C. U. Yurteri, S. Trigwell, S. De, and R. Sharma, Chem. Eng. Sci. **61**, 2192 (2006).
[2] A. J. Hickey, H. M. Mansour, M. J. Telko, Z. Xu, H. D. C. Smyth, T. Mulder, R. McLean, J. Langridge, and D. Papadopoulus, J. Pharm. Sci. **96**, 1302 (2007).
[3] Z. Xu, H. M. Mansour, and A. J. Hickey, J. Ad. Sci. Technol. **25**, 451 (2011).
[4] P. C. L. Kwok and H. K. Chan, J. Pharm. Pharmacol. **61**, 1587 (2009).
[5] X. Meng, J. Zhu, and J. Zhang, J. Phys. D **42**, 065201 (2009).
[6] A. Jaworek, W. Balachandran, A. Krupa, J. Kulon, and M. Lackowski, Environ. Sci. Technol. **40**, 6197 (2006).
[7] M. Khan, M. Schutyser, K. Schroen, and R. Boom, J. Food Eng. **111**, 1–5 (2012).
[8] B. Gady, D. Schleef, R. Reifenberger, D. Rimai, and L. P. DeMejo, Phys. Rev. B **53**, 8065 (1996).
[9] B. Gady, R. Reifenberger, D. Rimai, and L. P. DeMejo, Langmuir **13**, 2533 (1997).
[10] M. J. Bunker, M. C. Davies, M. B. James, and C. J. Roberts, Pharm. Res. **24**, 1165 (2007).
[11] J. Mahanty and M. T. Michalewicz, Aust. J. Phys. **40**, 413 (1987).
[12] T. Matsuyama, H. Yamamoto, and M. Washizu, J. Electrostat. **36**, 195 (1995).
[13] Y. Nakajima and T. Sato, J. Electrostat. **45**, 213 (1999).
[14] H. Zhou, M. Götzinger, and W. Peukert, Powder Technol. **135–136**, 82 (2003).
[15] T. Tang, C-Y. Hui, and A. Jagota, J. Appl. Phys. **99**, 054906 (2006).
[16] T. Matsuyama and H. Yamamoto, Part. Part. Syst. Charact. **24**, 79 (2007).
[17] E. Bichoutskaia, A. L. Boatwright, A. Khachatourian, and A. J. Stace, J. Chem. Phys. **133**, 024105 (2010).
[18] G. Arfken, "Bispherical coordinates," *Mathematical Methods for Physicists*, 2nd ed. (Academic Press, Orlando, FL, 1970), pp. 115–117.
[19] P. M. Morse and H. Feshbach, "Solutions of Laplace's and Poisson's equations," *Methods of Theoretical Physics, Part II* (McGraw-Hill, New York, 1953), p. 1298.
[20] H. T. Ochs III and R. R. Czys, Nature (London) **327**, 606 (1987).
[21] B. A. Tinsley, Rep. Prog. Phys. **71**, 066801 (2008).
[22] A. Khain, V. Arkhipov, M. Pinsky, Y. Feldman, and Y. Ryabov, J. Appl. Meteor. **43**, 1513 (2004).
[23] J. Israelachvili, *Intermolecular and Surface Forces* (Academic Press, London, 1998).
[24] A. J. Stace, A. L. Boatwright, A. Khachatourian, and E. Bichoutskaia, J. Colloid Interface Sci. **354**, 417 (2011).
[25] N. A. Burnham, R. J. Colton, and H. M. Pollock, Phys. Rev. Lett. **69**, 144 (1992).
[26] W. A. Ducker, T. J. Senden, and R. M. Pashley, Nature (London) **353**, 239 (1991).
[27] R. Mackel, H. Baumgartner, and J. Ren, Rev. Sci. Instrum. **64**, 694 (1993).
[28] R. Messina, J. Chem. Phys. **117**, 11062 (2002).
[29] T. Nguyen and S. Nieh, J. Electrostat. **22**, 213 (1989).